LAWRENCE
LIVERMORE
NATIONAL
LABORATORY

LLNL-JRNL-403277

Computational exploration of polymer nanocomposite mechanical property modification via cross-linking topology

N. Lacevic, R. Gee, A. Saab, R. Maxwell

April 29, 2008

Journal of Chemical Physics

Disclaimer

Computational exploration of polymer nanocomposite mechanical property modification via cross-linking topology

Naida Lacevic*, Richard H. Gee**, Andrew Saab, and Robert Maxwell
Lawrence Livermore National Laboratory, Livermore CA 94551

Abstract

Molecular dynamics simulations have been performed in order to study the effects of nanoscale filler cross-linking topologies and loading levels on the mechanical properties of a model elastomeric nanocomposite. The model system considered here is constructed from octa-functional polyhedral oligomeric silsesquioxane (POSS) dispersed in a poly(dimethylsiloxane) (PDMS) matrix. Shear moduli, *G*, have been computed for pure and for filled and unfilled PDMS as a function of cross-linking density, POSS fill loading level, and polymer network topology. The results reported here show that *G* increases as the cross-linking (covalent bonds formed between the POSS and the PDMS network) density increases. Further, *G* is found to have a strong dependence on cross-linking topology. The increase in shear modulus, *G,* for POSS filled PDMS is significantly higher than that for unfilled PDMS cross-linked with standard molecular species, suggesting an enhanced reinforcement mechanism for POSS. In contrast, in blended systems (POSS/PDMS mixture with no cross-linking) *G* was not observed to significantly increase with POSS loading. Finally, we find intriguing differences in the structural arrangement of bond strains between the cross-linked and the blended systems. In the unfilled PDMS the distribution of highly strained bonds appears to be random, while in the POSS filled system, the strained bonds form a net-like distribution that spans the network. Such a distribution may form a structural network "holding" the composite together and resulting in increases in *G* compared to an unfilled, cross-linked system.

* Corresponding author: nlacevic@consalteff.com
** Corresponding author: gee10@llnl.gov

These results are of importance for engineering of new POSS-based multifunctional materials with tailor-made mechanical properties.

Introduction

Polymer nanocomposite (PNC) materials (with sub-micron size fillers) are attractive alternatives to standard polymer composites (with micron size fillers) due to the possibility of tailoring their structure (and performance) on the nanoscale and with much greater chemical fidelity than is ordinarily possible for a standard composite. Advantageously, PNCs also may exhibit comparable or enhanced mechanical and physical properties to standard composites with a lower volume addition of filler, or produce properties not achievable with larger fillers.[1-8] For comprehensive reviews of recent trends, issues and advances in the field of PNC's see e.g. Refs. [9-11]

In this work we focus on a model PNC constructed from polyhedral oligomeric silsesquioxane (POSS) incorporated into a poly(dimethylsiloxane) (PDMS) elastomeric matrix. Such a nanocomposite might have broad potential application, ranging from supported catalytically active composites[12,13] to tissue engineering.[2,14,15] There have been numerous experimental,[13,16-21] theoretical and computational studies[22-30] that have dealt with the synthesis and characterization of the physical and mechanical properties of PNC materials as a function of changes to parameters. One of the common goals of studies regarding POSS/PDMS systems is to understand how the microscopic morphology of POSS incorporation into the polymer matrix influences the macroscopic properties.[31] To date, this has proven to be difficult to study in well-controlled laboratory experiments, but examples do exist. In one of the first successful demonstrations, Laine and co-workers[32] showed that certain arrangements of POSS in an epoxy composite could yield enhanced mechanical properties. While the ability to experimentally design POSS based nanocomposites with a known structure and desired properties is still a challenge, computer

simulations are a useful tool to systematically and qualitatively investigate how structure, POSS functionality, and incorporation into a polymer matrix influence performance. For example, Lamm *et al*.,[25] showed that a variety of structures could be produced by changing tether length, component interactions, and POSS concentrations, suggesting that a significant improvement in tailorability could be achieved.[25]

One of the most intriguing unresolved issues for PNCs is understanding the reinforcement effects of nanofillers in polymer networks on the molecular level.[33] Recent work of Mark *et al*. [34] showed that it is not enough to physically blend POSS and PDMS in order to obtain reinforcement. It was necessary, rather, to incorporate POSS as pendants off the PDMS chains or to crosslink PDMS through the POSS units via tetra-functional POSS particles in order to achieve significant effect on the nanocomposite's mechanical properties.[34] Since one can envision a variety of configurations in which the POSS fillers may be bonded, or cross-linked, to the polymer matrix, we investigate: (1) the effect of cross-linking topology on the mechanical properties of polymer nanocomposites, (2) the extent to which nano-filler loading and amount of cross-linking complement each other in tailoring nanocomposite mechanical properties, and (3) the reinforcement of POSS filled PDMS in comparison to cross-linked unfilled PDMS.

Simulation Model and Method

Our goal is to obtain qualitative insights into the effects of the addition of cross-links to polymer nanocomposites. As such, we are concerned with capturing the general features of filled polymer systems rather than exactly reproducing experimental observables (e.g., shear modulus of a POSS-PDMS nanocomposite). PDMS molecules are represented using the force field developed by Frischknecht and Curro[35], which is also implemented for the POSS nanofiller interactions. POSS

molecules are functionalized with 8 butyl tethers. Hydrogen atoms are not modeled explicitly. The methyl groups on POSS and PDMS are treated as united atoms. The same force fields are used in a series of papers by Striolo, *et al*.[22-24,36] where the authors were investigating thermodynamic and transport properties of POSS filled PMDS systems. Snapshots of a POSS cage, a PDMS chain of molecular weight of 8,800, and non-cross-linked POSS filled PDMS at 3% and 10 % POSS loading are shown in Figure 1*a–d*, respectively. The system preparation, equilibration, and POSS loading information are provided in the Appendix below. All simulations are performed with LAMMPS.[37]

Results and Discussions

It is well known that the mechanical properties of nanocomposites are strongly affected by nanofiller dispersion and agglomeration.[38] In order to gain an understanding of the probability for POSS to disperse well and/or agglomerate in PDMS, we have performed a series of MD calculations to compute the POSS-POSS interaction potential energy, U_p, the corresponding fluctuation in potential energy δU_p, and the specific heat $C_p = \frac{\left\langle \delta U^2{}_p \right\rangle}{T^2}$, where $\delta U_p = U_p - \left\langle U_p \right\rangle$, T is temperature, and $\langle\ \rangle$ represents an ensemble average. (Note that C_p is a specific heat per POSS molecule.) Both U_p and C_p have been computed from the non-bonded energy contribution to the force field, and therefore depend only on the POSS-POSS distance. Similar dispersion characterization has been performed by Starr[39] *et al*. for polyhedral nanoparticles in a dense bead-spring polymer melt. As noted in Ref. [39], U_p and C_p are sensitive to the distance between nanofillers, and therefore can be used to determine an approximate boundary between dispersed and agglomerated states, further, these quantities provide a relatively simple metric for dispersion which are more easily determined experimentally then other known metrics, e.g., the structure factor, *S(q)*. In the limiting cases of low and high nanofiller loadings, where the system achieves a stable phase,

U_p was predicted to exhibit less fluctuation compared to U_p at intermediate nanofiller loading.[39] Results of our MD calculations of U_p and C_p as a function of POSS loading are shown in Figures 2*a* and 2*b,* respectively, and show trends similar to those predicted in Ref. [39]. U_p monotonically decreases with increased POSS loading indicating that POSS molecules, on average, are closer to each other, as would be expected. We observe a maximum in C_p between 10 % and 30 % of POSS loading indicating an approximate bound between a dispersed and agglomerated state could be anywhere in the aforementioned interval.

The effects of cross-linking topology on mechanical properties of the nanocomposite were investigated through simulations of three cross-linking schemes between the POSS and PDMS. In topology I (TI) only the terminal methyl groups on the PDMS chains were allowed to cross-link, as illustrated in Figure 3*a*. In this topology, both sets of CH_3 groups at PMDS chain ends could cross-link with free tether ends on a POSS molecule. In topology II (TII), all CH_3 side groups on the PDMS chains were allowed to cross-link with free POSS tether ends, as illustrated in Figure 3*b*. Topology III (TIII) allowed only *one* terminal CH_3 group at the end of each PMDS chain end to cross-link to a POSS tether end, as illustrated in Figure 3*c*. We selected these particular topologies on the basis that PDMS polymers allowing the attachment of up to one POSS molecule per silane repeat unit are readily available from commercial sources. Therefore, these topologies best reflect actual materials that are most easily synthesized, thereby allowing for some empirical testing of our computational results. The cross-linked configurations were produced from well-equilibrated, physically mixed systems with the desired loading fraction (see Appendix for details). A basic cross-linking algorithm was used to compute all distances between CH_3 groups on PDMS and POSS tethers. A list of allowed CH_3 pairs was kept for those pairs within a certain cutoff distance of 2.5 nm. Each CH_3 group was allowed to participate in only one cross-link, and any given POSS

molecule and PDMS chain were constrained to only link together once. The list of CH_3 pairs was randomized and bonds were formed from a chosen fraction of eligible CH_3 pairs. The cross-linking bond was characterized by an equilibrium length of *0.53 nm* and stiffness constant of 146.4×10^3 $kJ/(mol\ nm^2)$ (similar to the stiffness of the C-C bond). We note that our cross-linking scheme is oversimplified compared to the complex chemistry involved in the synthesis of real POSS-PDMS networks. Our goal is not to simulate exact cross-linking chemistry but to create different topologies for cross-linking and gain insights into the resulting mechanical properties.

The effects of the topology and the average number of cross-links per POSS, N_X, on the calculated shear modulus, *G,* are shown in Figure 4*a-d* for POSS loadings of *3*, *5*, *10* and *20%,* respectively. Note that *G* is computed from a linear fit of shear stress (σ) vs. true strain (γ). An example of such a fit is shown in Figure 4*b*. The correlation coefficients for each fit were between 0.8 and 0.98. The shear moduli vs. POSS loading were markedly different for the three topologies. In Topology I with a 3% POSS loading (Figure 3*a*), an increase in *G* was observed for $N_X > 4$. This is likely because both CH_3 groups on one PDMS end can each link to different POSS cages. This could lead to a network connection where two POSS cages are linked via PDMS chain ends, essentially creating a POSS network. This is in general agreement with findings reported by Pan, *et al.,*[34] where evidence for a reinforcing effect of linking nanofillers such as tetra-POSS particles was observed.[40,41] In contrast, *G* does not show any increase for topologies TII and TIII at 3% POSS loading due to the fact that the low POSS concentration relative to the concentration of available PDMS methyl groups yields a low number of POSS-to-POSS cross-linking sites, and therefore, network formation is not efficient.

At 5% POSS loading (Figure 4*b*), it was observed that as N_X increased to values greater than *4*, *G* increased sharply for topology TI, for similar reasons as in the 3% POSS loading, above. The shear modulus, *G*, was also observed to increase in Topology TII for $N_X > 4$, although more gradually as compared to TI. This is due to the increased number of cross-linking sites available for POSS compared to topology TI, which results in longer more compliant segments between POSS cages. Topology TII is likely to produce a network resembling a "spider web" in which each node could be replaced with a POSS cage and PDMS chains (along with the butyl tethers) serve as connecting "silk". Only negligible changes in *G* were observed in case of topology TIII, which imposes the strictest conditions on POSS-PDMS linking (one terminal CH_3 group to one POSS tether). TIII minimizes the connectivity and increases the probability of forming unconnected, non-load bearing regions, e.g., "dumbbells" (PDMS chains with one POSS attached to each end). Topology TIII also guarantees long, flexible segments between POSS cages that are not tightly bound to the network.

At 10 and 20% loading (Figures 4*c* and *d*, respectively), TI and TII were the only topologies that produced significant increases in *G*. For topology TIII, the PDMS chain ends are the limiting species for cross-linking at these higher POSS loadings. For topology TII, at higher loadings, *G* was observed to increase for lower values of N_X than observed for low POSS loadings likely because of a surplus of POSS tethers that can be cross-linked with CH_3 on the PDMS chains and thus leading to more efficient network formation.

These observations point to the importance of developing a deeper understanding of the cross-linking structure of filler/polymer networks beyond basic metrics such as cross-linking density. It is natural to ask what is the origin of the increase in shear modulus in the POSS-PDMS network for each cross-linking topology. One possible explanation (in the case of topology TII, at least) is the

effective reduction of molecular mass between cross-links, $M_{x-links}$, which would be expected to raise the modulus since $G \sim \frac{1}{M_{x-links}}$.[42] In the cases of topologies TI and TIII, however, the cross-linking is done only at the PDMS ends. Therefore there is no reduction in $M_{x-links}$, nevertheless we note an increase in G for increased POSS loading (e.g., at 5% and 10% POSS loading for topology TI at $N_x > 4$) suggesting another mechanism is involved.

In order to better address the question of how $M_{x\text{-}links}$ influences the shear modulus, we focus on topology TII since it produced increases in G at each loading. The average molecular weight of segments between cross-links, $M_{x\text{-}links}$, was computed for each POSS loading case, including unfilled PDMS with and without chain-to-chain cross-linking. Increasing the number of cross-links decreases $M_{x\text{-}links}$. Figure 5 shows G vs $1/M_{x\text{-}links}$ for unfilled PDMS at 3, 5, 10 and 20% POSS loading for topology TII. The shear modulus for the filled topology TII systems are significantly higher than those for the unfilled system at similar molecular weights between cross-links, indicating a substantial stiffness enhancement provided by POSS beyond serving as a location for cross-linking.

In order to gain understanding into the origin of this enhanced reinforcement, individual bond energies for the system under shear were computed. After shearing, thermal fluctuations were eliminated by energy minimizing the systems, and then computing the energy of each bond. All particles were then sorted according to their share of bonding energies and a subset of particles with the highest bond energies were extracted. These particles form bonds with a high degree of strain. Figure 6 shows POSS filled PDMS (Figure 6*a*) and unfilled PDMS (Figure 6*b*) where these localized high strain bonds are colored in orange. The distribution of strained bonds for each case is

strikingly different. It appears that POSS induces the formation of a "mesh" like structure, while in the unfilled PDMS system the distribution appears random. This difference in structure may be related to observed enhancement in *G* in the case of POSS filled systems because of the formation of the continuous load bearing network of strained bonds that is absent in unfilled PDMS.

Conclusions

Molecular dynamics simulations have been implemented to study the effects of cross-linking topologies and POSS loading in POSS-PDMS nanocomposites. POSS loading, average number of cross-links per POSS and cross-linking topologies were varied systematically and shear modulus computed for each case. We find that significant increases in shear modulus can be achieved via high POSS loadings with cross-link topologies in which *2* or more POSS tethers are linked to the polymer matrix. We demonstrate that both loading and cross-linking scheme can be used in synergy to tailor nanocomposite mechanical properties. We also show significant differences in the structural arrangement of highly strained bonds between unfilled PDMS and POSS loaded PDMS indicating mechanisms of enhanced reinforcement for filled nanocomposites beyond cross-linking of the polymer matrix. These results are of importance in designing new polymer nanocomposites containing linked fillers.

Acknowledgements

We thank to Ticora Jones, Thomas Wilson, and Theodore Baumann for helpful discussion on POSS PDMS synthesis. This work is supported in part by the Transformational Materials Initiative (TMI) Laboratory Directed Research and Development (LDRD) grant, 06-SI-005. This work is performed

under the auspices of the U.S. Department of Energy by Lawrence Livermore National Laboratory under Contract DE-AC52-07NA27344.

APPENDIX

System preparation and equilibration. The POSS loading, *Wt*, is determined using the formula $Wt = \frac{N_{POSS}\ M_{POSS}}{N_{POSS}\ M_{POSS} + N_{PDMS}\ M_{PDMS}}$, where M_{POSS} = 872 *g/cc* and M_{PDMS} = 8,800 *g/cc* are the molecular weights of POSS and PDMS, respectively, and N_{POSS} and N_{PDMS} are the numbers of POSS and PDMS molecules respectively. *Wt* is given in the first column of Table 1. Unit cells composed of POSS cages and PDMS chains at desired loadings are created at low density. The number of POSS cages and PDMS chains for each unit cell is provided in parentheses after the loading percent, *Wt*, in the first column of Table 1 (e.g., *1 (1;8)* means *1*% POSS loading with a unit cell containing *1* POSS cage and *8* PDMS chains). The cubic unit cell is further replicated in three directions to obtain a final "super-cell" simulation box. The replication factor, *R*, is given in the second column. Each number corresponds to replication in one direction (e.g., 444 means the unit cells was replicated *4* times in *x*, *4* times in *y* and *4* times in *z* directions).

Equilibration is performed in the *NPT* ensemble at zero pressure and *600 K*. After equilibration at high temperature, the system is cooled down to *300 K* in increments of *50 K*. At each temperature, the system is equilibrated for at least *5 ns*. The equilibrium cubic box length, *L*, and density, ρ, at 300 K is provided in the fifth and sixth column of Table 1, respectively. The computed bulk modulus, *K*, is given in the eighth column. We observed only slight increases in bulk modulus as POSS loading is increased. A similar trend is observed in shear modulus, *G*, after POSS-PDMS nanocomposite equilibration in the absence of cross-links. We introduce three cross-linking scenarios described in the Results and Discussion section. For each system where cross-linking is introduced, the equilibrium cross-link bond length is gradually decreased from 2.5 nm to 0.53 nm,

and the system is equilibrated at zero pressure until the total energy of the system reaches the steady state.

Chain flexibility: Characteristic ratio, C_n. In order to characterize local bond conformations in PDMS chains, we compute the characteristic ratio, C_n, as a function of POSS loading. The comparison of the computed values of C_n for our model and experimental values that are available for various flexible polymers is an important metric that quantifies how POSS inclusion alters the statistical behavior of conformationally disordered polymer chains. We compute the characteristic ratio as,

$$C_n = \frac{\langle R^2 \rangle}{nl^2}, \tag{5}$$

where $\langle R^2 \rangle$ is the mean-square end-to-end distance, n is the number of bonds on a single chains, l is the Si-O bond length (1.64 *nm*), and C_∞ is the characteristic ratio for infinitely long chains extrapolated from Eq. (5) as n $\rightarrow \infty$. Figure 7*a* shows C_∞ for the neat PDMS system and PDMS with several POSS loadings (no cross-links are introduced). The experimental values of C_∞ for the unfilled PDMS are in the range of 5.5 to 7.8,[43] depending on the solvent and temperatures. We do not observe significant change in C_∞ as POSS loading increases suggesting that conformations of the PDMS chains are not significantly affected by POSS insertion.

We have further verified that there is not significant sample to sample variation in C_∞ as shown by the computed values of C_∞ for 5 independent configurations at 5% POSS loading and no cross-links (Figure 7*b*).

REFERENCES

(1) Ear, Y.; Silverman, E. *Mrs Bulletin* **2007**, *32*, 328.

(2) Hule, R. A.; Pochan, D. J. *Mrs Bulletin* **2007**, *32*, 354.

(3) Hunter, D. L.; Kamena, K. W.; Paul, D. R. *Mrs Bulletin* **2007**, *32*, 323.

(4) Krishnamoorti, R. *Mrs Bulletin* **2007**, *32*, 341.

(5) Luo, J. J.; Daniel, I. M. *Composites Science And Technology* **2003**, *63*, 1607.

(6) Schadler, L. S.; Kumar, S. K.; Benicewicz, B. C.; Lewis, S. L.; Harton, S. E. *Mrs Bulletin* **2007**, *32*, 335.

(7) Soong, S. Y.; Cohen, R. E.; Boyce, M. C. *Polymer* **2007**, *48*, 1410.

(8) Winey, K. I.; Kashiwagi, T.; Mu, M. F. *Mrs Bulletin* **2007**, *32*, 348.

(9) Hussain, F.; Hojjati, M.; Okamoto, M.; Gorga, R. E. *Journal Of Composite Materials* **2006**, *40*, 1511.

(10) Pielichowski, K.; Njuguna, J.; Janowski, B.; Pielichowski, J. Polyhedral oligomeric silsesquioxanes (POSS)-containing nanohybrid polymers. In *Supramolecular Polymers Polymeric Betains Oligomers*, 2006; Vol. 201; pp 225.

(11) Li, G. Z.; Wang, L. C.; Ni, H. L.; Pittman, C. U. *Journal Of Inorganic And Organometallic Polymers* **2001**, *11*, 123.

(12) Waddon, A. J.; Zheng, L.; Farris, R. J.; Coughlin, E. B. *Nano Letters* **2002**, *2*, 1149.

(13) Zheng, L.; Farris, R. J.; Coughlin, E. B. *Macromolecules* **2001**, *34*, 8034.

(14) Kannan, R. Y.; Salacinski, H. J.; De Groot, J.; Clatworthy, I.; Bozec, L.; Horton, M.; Butler, P. E.; Seifalian, A. M. *Biomacromolecules* **2006**, *7*, 215.

(15) Kannan, R. Y.; Salacinski, H. J.; Butler, P. E.; Seifalian, A. M. *Accounts Of Chemical Research* **2005**, *38*, 879.

(16) Liu, H. Z.; Zheng, S. X. *Macromolecular Rapid Communications* **2005**, *26*, 196.

(17) Leu, C. M.; Chang, Y. T.; Wei, K. H. *Macromolecules* **2003**, *36*, 9122.

(18) Pittman, C. U.; Li, G. Z.; Ni, H. L. *Macromolecular Symposia* **2003**, *196*, 301.

(19) Fu, B. X.; Zhang, W. H.; Hsiao, B. S.; Rafailovich, M.; Sokolov, J.; Johansson, G.; Sauer, B. B.; Phillips, S.; Balnski, R. *High Performance Polymers* **2000**, *12*, 565.

(20) Pyun, J.; Matyjaszewski, K. *Macromolecules* **2000**, *33*, 217.

(21) Shockey, E. G.; Bolf, A. G.; Jones, P. F.; Schwab, J. J.; Chaffee, K. P.; Haddad, T. S.; Lichtenhan, J. D. *Applied Organometallic Chemistry* **1999**, *13*, 311.

(22) Striolo, A.; McCabe, C.; Cummings, P. T. *Journal Of Chemical Physics* **2006**, *125*.

(23) Striolo, A.; Chialvo, A. A.; Cummings, P. T.; Gubbins, K. E. *Journal Of Chemical Physics* **2006**, *124*.

(24) Striolo, A.; McCabe, C.; Cummings, P. T. *Macromolecules* **2005**, *38*, 8950.

(25) Lamm, M. H.; Chen, T.; Glotzer, S. C. *Nano Letters* **2003**, *3*, 989.

(26) Smith, G. D.; Bedrov, D.; Li, L.; O, B. *Journal Of Chemical Physics* **2002**, *117*, 12.

(27) Peng, Y.; McCabe, C. *Molecular Physics* **2007**, *105*, 261.

(28) Patel, R. R.; Mohanraj, R.; Pittman, C. U. *Journal Of Polymer Science Part B-Polymer Physics* **2006**, *44*, 234.

(29) Bharadwaj, R. K.; Berry, R. J.; Farmer, B. L. *Polymer* **2000**, *41*, 7209.

(30) Gersappe, D. *Physical Review Letters* **2002**, *89*, 4.

(31) Haddad, T. S.; Lichtenhan, J. D. *Macromolecules* **1996**, *29*, 7302.

(32) Zhang, C. X.; Babonneau, F.; Bonhomme, C.; Laine, R. M.; Soles, C. L.; Hristov, H. A.; Yee, A. F. *Journal Of The American Chemical Society* **1998**, *120*, 8380.

(33) Mark, J. E.; Erman, B. *Rubberlike Elasticity*; Cambridge University Press: Cambridge, UK, 2007.

(34) Pan, G. R.; Mark, J. E.; Schaefer, D. W. *Journal Of Polymer Science Part B-Polymer Physics* **2003**, *41*, 3314.

(35) Frischknecht, A. L.; Curro, J. G. *Macromolecules* **2003**, *36*, 2122.

(36) Striolo, A.; McCabe, C.; Cummings, P. T. *Journal Of Physical Chemistry B* **2005**, *109*, 14300.

(37) Plimpton, S. J. *Journal Of Computational Physics* **1995**, *117*, 1.

(38) Heinrich, G.; Kluppel, M. Recent advances in the theory of filler networking in elastomers. In *Filled Elastomers Drug Delivery Systems*, 2002; Vol. 160; pp 1.

(39) Starr, F. W.; Douglas, J. F.; Glotzer, S. C. *Journal Of Chemical Physics* **2003**, *119*, 1777.

(40) Choi, J.; Harcup, J.; Yee, A. F.; Zhu, Q.; Laine, R. M. *Journal Of The American Chemical Society* **2001**, *123*, 11420.

(41) Laine, R. M.; Choi, J. W.; Lee, I. *Advanced Materials* **2001**, *13*, 800.

(42) Treloar, L. R. G. *The Physics of Rubber Elasticity*, 3rd ed.; Clarendon Press: Oxford, 1975.

(43) Flory, P. *Statistical Mechanics of Chain Molecules*; Interscience: New York, 1969.

(44) Dattelbaum, D. M.; Jensen, J. D.; Schwendt, A. M.; Kober, E. M.; Lewis, M. W.; Menikoff, R. *Journal of Chemical Physics* **2005**, *122*.

Table 1. Loading information for POSS-PDMS nanocomposite considered in this work. POSS percent loading, *Wt*, unit cell replication factor, *R*, number of POSS cages, number of PDMS chains, equilibrium box length, *L*, equilibrium density ρ, total number of atoms, and bulk modulus, *K*. Note that K does not significantly increase as POSS loading increases in the case of physical mixture of POSS and PDMS. The value of *K* for unfilled PDMS is similar to the value found in Ref. [44].

Wt [%]	*R*	*# Cages*	*# Chains*	*L* [Å]	ρ [g/cc]	*# Atoms*	*K [GPa]*
PDMS	444	0	64	97.400	1.0215	30,720	0.952
1 (1; 8)	223	12	96	112.180	1.0087	46,704	0.9409
2 (1; 4)	333	27	108	117.144	1.0082	53,244	0.9276
3 (1; 3)	424	32	96	112.899	1.0092	47,744	0.9332
5 (1; 2)	443	48	96	113.463	1.0099	48,576	0.9371
10 (1; 1)	454	80	64	108.310	1.0126	42,560	0.9436
20 (3; 1)	444	132	64	105.869	1.0228	40,704	0.9787

List of Figure Captions:

Figure 1. Snapshots from our simulations of (*a*) Butyl octa-functional POSS molecule ("reactive" methyl groups are labeled in blue), (*b*) PDMS chain, (*c*) 3% POSS loading dispersed in PDMS at 300 K, and (*d*) 10% POSS loading dispersed in PDMS at 300 K. Note that in (*c*) and (*d*) PDMS chains are colored purple and decreased in size in order to emphasize structural arrangement of POSS cages.

Figure 2. Dispersion of POSS-PDMS as a function of POSS loading as shown by: (*a*) Average POSS-POSS potential energy, U_p. (*b*) Specific heat C_p. The approximate bound between dispersive and agglomerated states is between 10% and 30% (by weight).

Figure 3. Cross-linking topologies: (*a*) Only the end (terminal) methyl groups on the PDMS chains are allowed to cross-link (note: both PDMS terminal methyl groups can cross-link with free POSS tether ends.) Black lines represent "bonds" between POSS tethers and PDMS ends and they are exaggerated in size. (*b*) Any methyl groups on the PDMS chains are allowed to cross -link with free POSS tether ends. (*c*) Only *one* end methyl group per PDMS chain end is allowed to cross-link. Note that length of chains (represented in red), POSS tethers (represented in yellow) and cross-links (represented in blue and black) are not to scale.

Figure 4. Shear modulus, G, as a function of number of cross-linking bonds, N_X, for topologies TI (black circles), TII (red squares), and TIII (green diamonds) at (*a*) 3%, (*b*) 5%, (*c*) 10% and (*d*) 20% POSS loading. Inset in panel (*b*) shows the shear stress vs. true strain at N_X = 4.58 and 6.25 and linear fits. Mechanical properties are markedly different for three topologies.

Figure 5. Shear modulus, G, vs. inverse molecular mass between cross-links, $M_{x\text{-}links}$, for unfilled PDMS system and 3, 5, 10 and 20% POSS loading. The POSS filled PDMS has significantly higher shear modulus compared to unfilled PDMS at comparable $M_{x\text{-}links}$.

Figure 6. Snapshots of the (*a*) POSS filled PDMS and unfilled PDMS (*b*) at Wt = 10 % under strain and $M_{x\text{-}links}$ = 450 g/mol. Particles with highest bond energies colored orange. These particles appear to form a "mesh" like structure for the filled system while the arrangement of aforementioned particles in the unfilled system appears random. The snapshots are shown for topology II.

Figure 7. (*a*) Characteristic ratio as a function of POSS loading (black circles). (*b*) Characteristic ratio for independent configurations at 5% POSS loading (black squares). The analysis is performed on systems without cross-links.

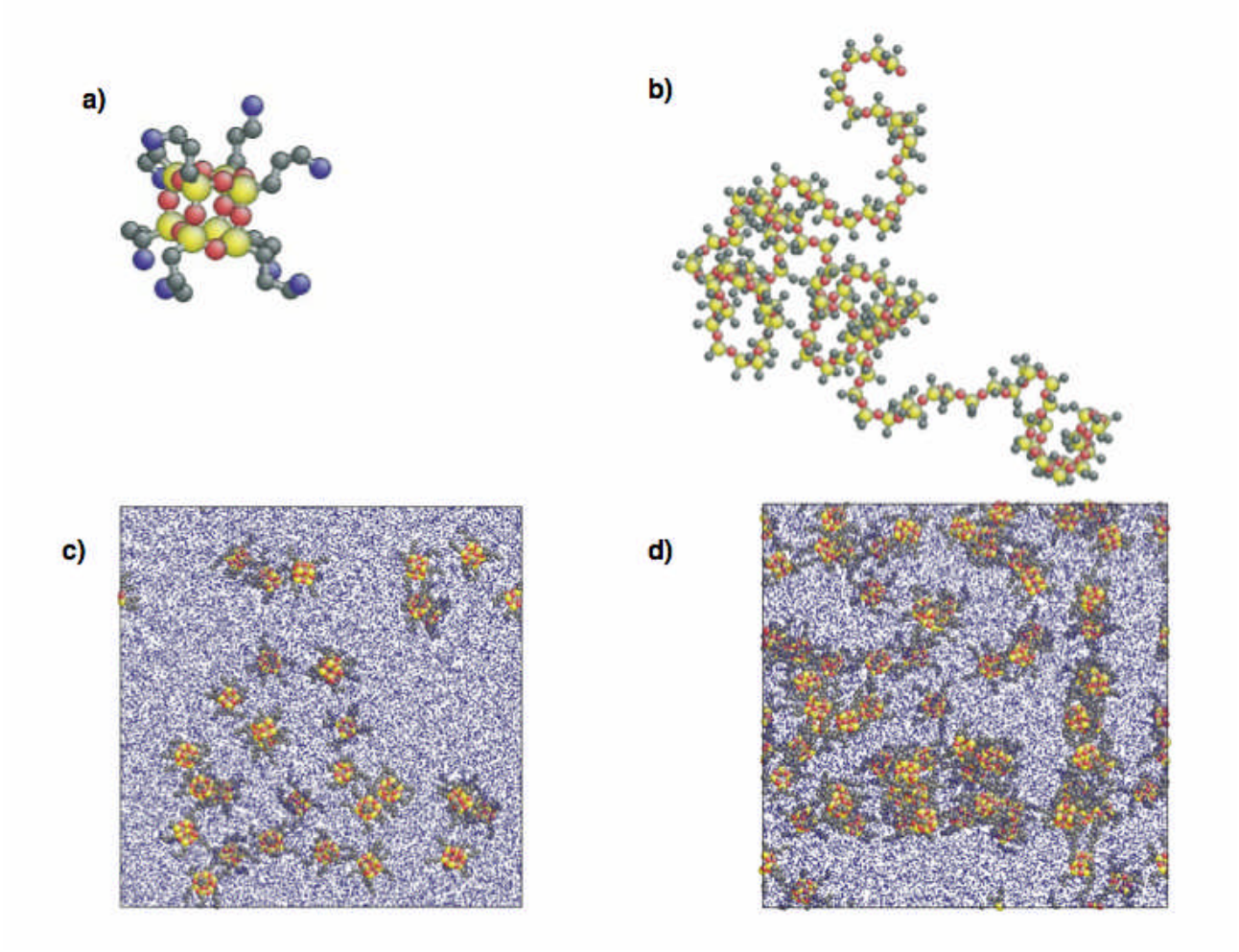

Figure 1

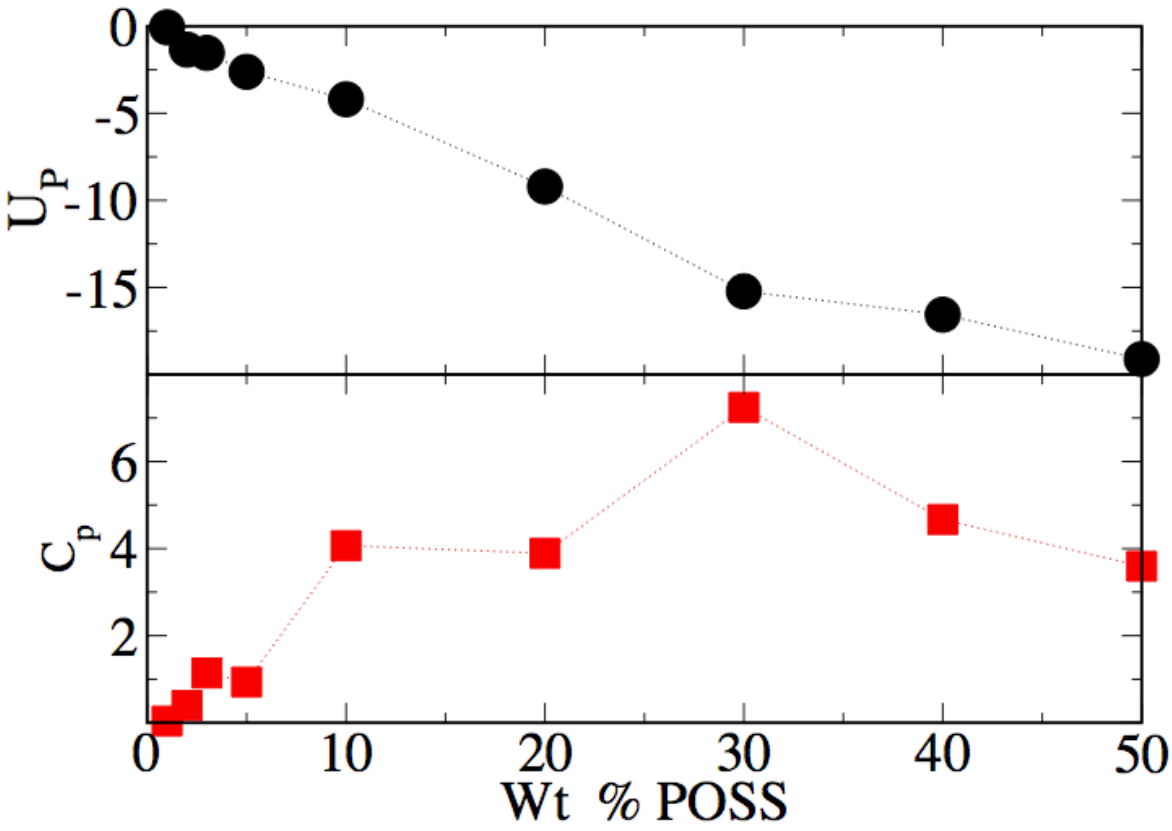

Figure 2

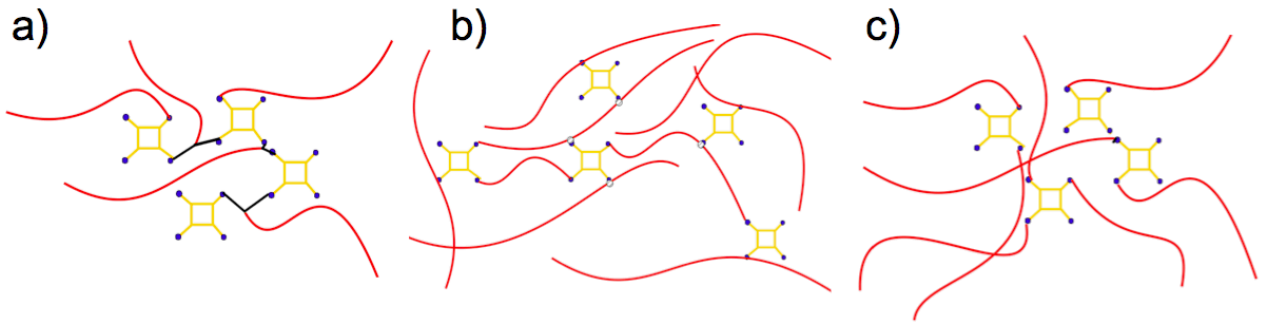

Figure 3

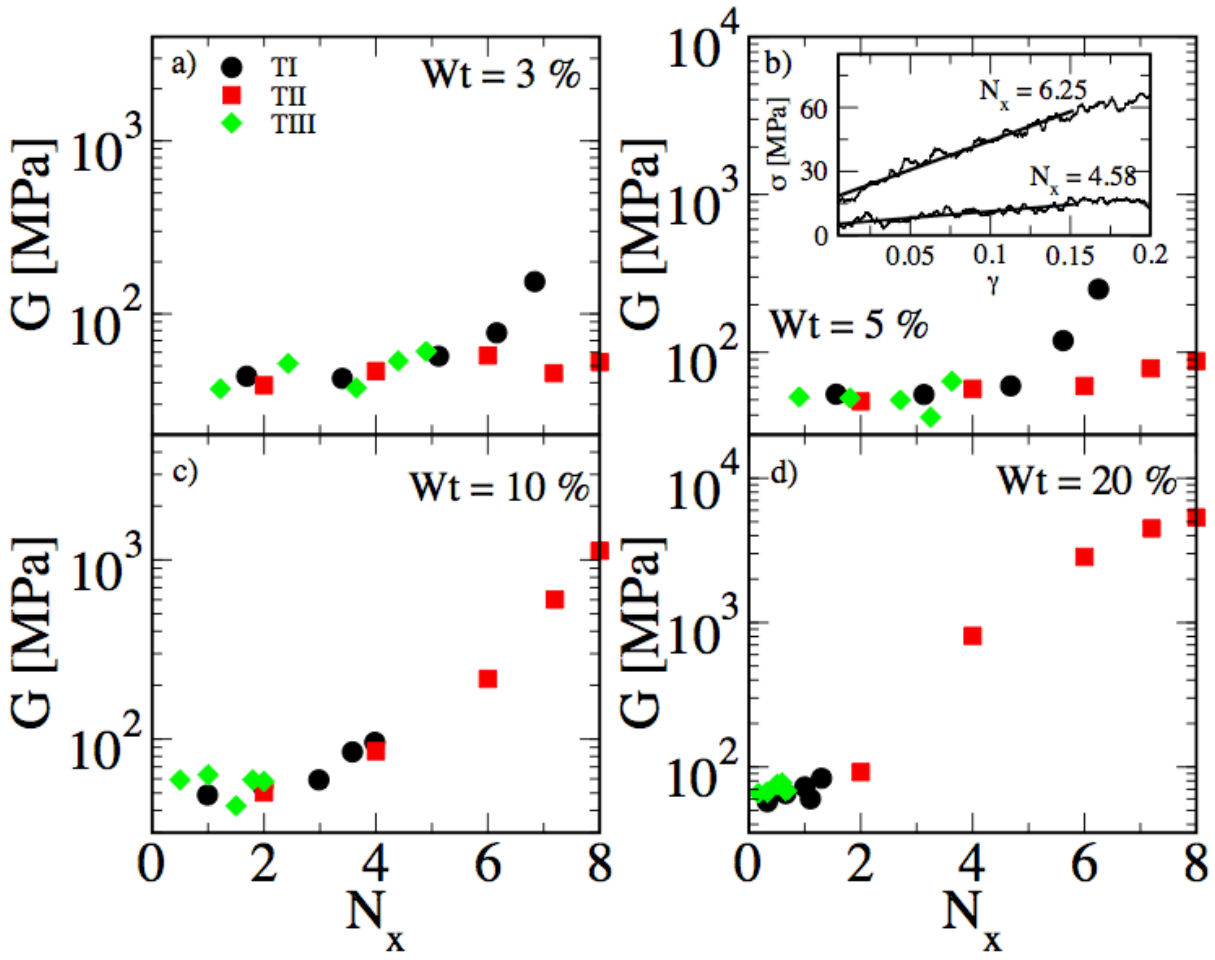

Figure 4

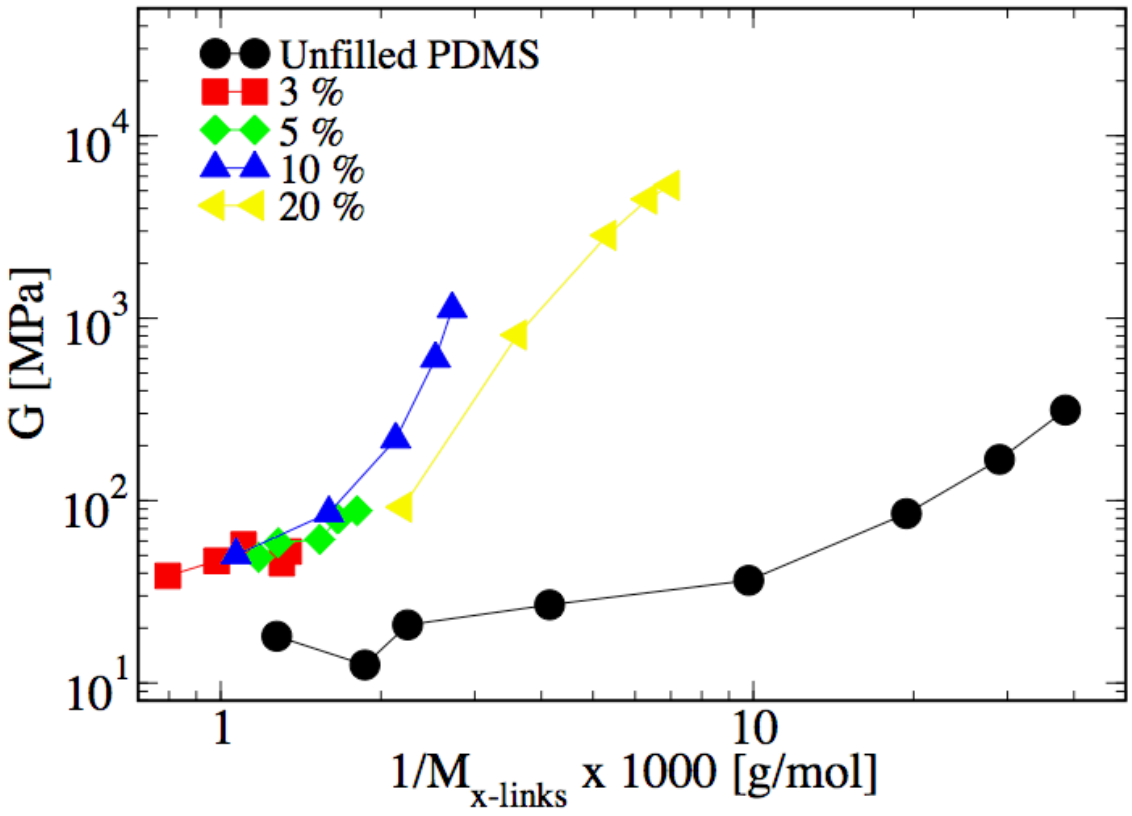
Unfilled PDMS
3 %
5 %
10 %
20 %
G [MPa]
10^4
10^3
10^2
10^1
1
10
$1/M_{x\text{-links}}$ x 1000 [g/mol]

Figure 5

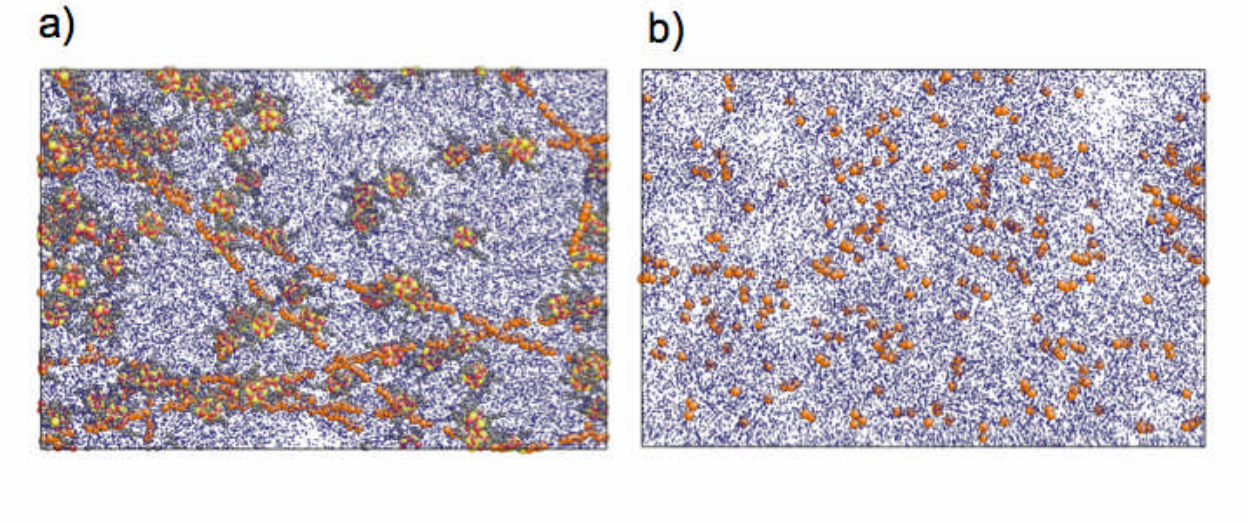

Figure 6

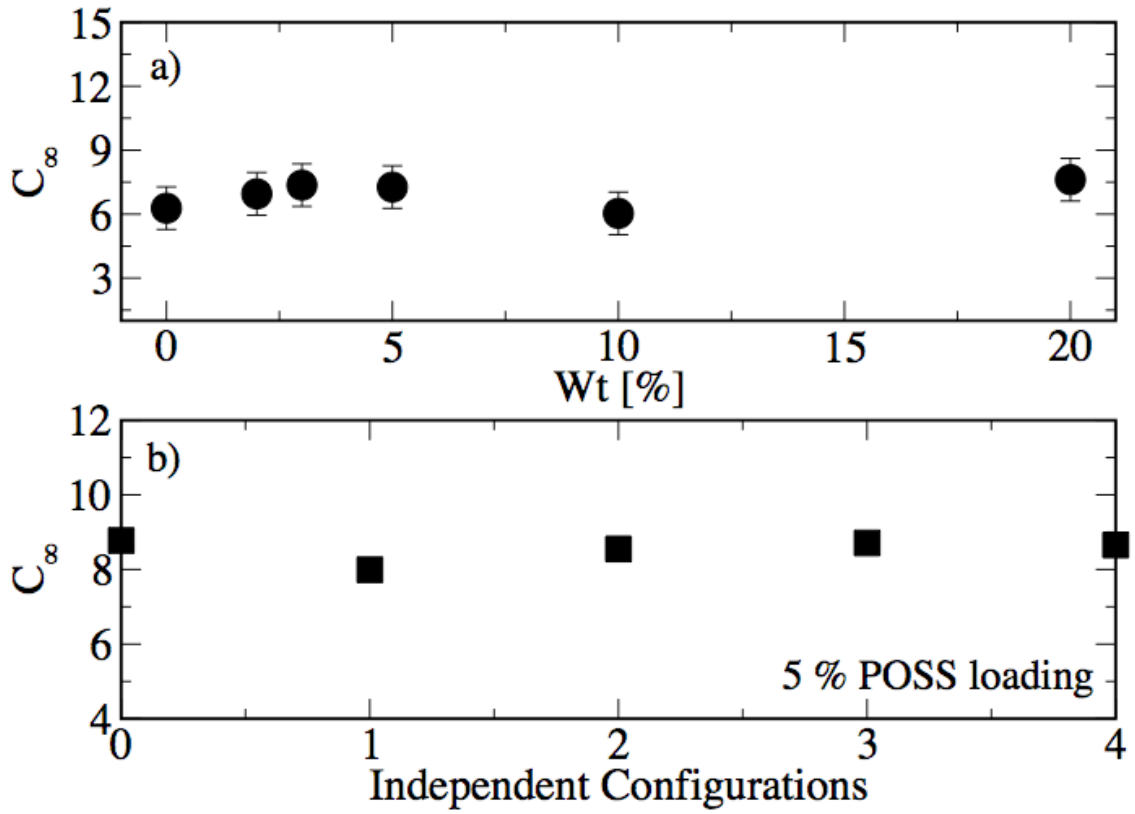

Figure 7